

A STUDY OF HYDRAULIC PROPERTIES IN A SINGLE FRACTURE WITH IN-PLANE HETEROGENEITY: AN EVALUATION USING OPTICAL MEASUREMENTS OF A TRANSPARENT REPLICA

ATSUSHI SAWADA* and HISASHI SATO

Geological Isolation Research and Development Directorate, Japan Atomic Energy Agency
4-33 Muramatsu Tokai-mura, Naka-gun, Ibaraki, 319-1194, Japan

*Corresponding author. E-mail : sawada.atsushi@jaea.go.jp

Received January 6, 2010

Experimental examinations for evaluating fractures were conducted by using transparent replicas of a single fracture in order to obtain the fracture data to contribute to the methodology on how to improve the definition of representative parameter values used for a parallel plate fracture model. Quantitative aperture distribution and quantitative tracer concentration data at each point in time were obtained by measuring the attenuation of transmitted light through the fracture in high spatial resolution. The representative aperture values evaluated from the multiple different measurement methods, such as arithmetic mean of aperture distribution measured by the optical method, transport aperture evaluated from the tracer test, and average aperture evaluated from the fracture void volume measurement converged to a unique value that indicates the accuracy of this experimental study. The aperture data was employed for verifying the numerical simulation under the assumption of Local Cubic Law and showed that the calculated flow rate through the fracture is 10% – 100% larger than hydraulic test results. The quantitative tracer concentration data is also very valuable for validating existing numerical code for advection dispersion transport in-plane heterogeneous fractures.

KEYWORDS : Fracture Aperture, Transmissivity, Transparent Replica, Optical Method, Local Cubic Law

1. INTRODUCTION

Understanding hydraulic and solute transport behavior in void space in underground is critical for the safety assessment of high-level radioactive waste disposal. In the case of crystalline rock, such as granite, groundwater flow is dominated by faults and fractures due to the very fine void space, small porosity, and low permeability of the rock matrix. From the macroscopic view, the interconnecting network structure is imperative to evaluating hydraulic properties. In frequent practice, a parallel plate model approximately representing a discrete fracture is applied to groundwater flow and nuclide transport assessment [1]. However, in reality, fracture surfaces are very rough and fracture apertures are unevenly distributed. The resulting heterogeneity strongly affects groundwater flow and solute transport within fractures. A parallel plate model requires representative values for transmissivity, aperture, etc. There are several definitions for representative fracture aperture based on this kind of model [2,3]. One can be calculated by the cubic law, with transmissivity obtained from hydraulic tests, called “hydraulic aperture”

or “cubic law aperture.” The other can be estimated from tracer test results, the “mass balance aperture.” In the case of true parallel plate fracture, these two values as defined above are then identical. Natural fractures, which have heterogeneous geometries, take on significantly different values. Therefore, the methodology for improving how we define representative parameter values used for a parallel plate model should be required as one of the relevant issues for developing more reliable safety assessments. It is known that the hydraulic aperture is usually smaller than the arithmetic mean of the geometric aperture distribution due to the heterogeneous distribution of fracture aperture[2]. Moreover, the arithmetic mean aperture as a representative aperture used for parallel plate modeling purposes might overestimate the Darcy flux.

Various methods for calculating representative aperture values, such as hydraulic aperture and mass-balance aperture, have been reported in the past [4-6]. Smith and Freeze (1979) [7] and Dagan (1979)[8] reported that the hydraulic aperture can be represented by the geometric mean of the aperture if the aperture is randomly distributed in space corresponding to the lognormal

distribution. Since a natural fracture shows more complicated geometry and aperture distribution, the numerical simulations created by using measured geometrical aperture distributions, assuming that local transmissivity is estimated from the cubic law by aperture at each point (the so-called Local Cubic Law, LCL), have been used to evaluate the representative aperture value. However, the applicability of LCL has been widely discussed. Nicholl et al. (1999)[9] employed a light-transmitted technique to measure aperture distribution at spatially high resolution for a fracture made by 15 cm by 30 cm transparent textured glass plates, and they also conducted hydraulic tests. The discharge rate calculated from two-dimensional Darcy-based flow simulation, with heterogeneous transmissivity distribution from the measured aperture distribution based on LCL, was 1.4 times larger than the hydraulic test result. Konzuk and Kueper (2004) [10] also reported that the two-dimensional Darcy flow simulations, based on LCL, estimate a flow rate that is about 1.75 times larger than hydraulic tests at fractures artificially induced in 20.3 cm by 25 cm of limestone sample. Aperture distributions were measured at cross sections at each sliced specimen perpendicular to a fracture in 5 mm spacing after impregnating resin into a fracture to prevent disturbance during slicing. For natural fractures, Hakami and Larsson (1996)[11] investigated a 19 cm by 41 cm large-scale granite core sample including a natural single fracture by applying hydraulic tests and measuring aperture distribution every 13 mm within a sliced rock sample. They found that the LCL model overestimates the hydraulic-test discharge rate by a factor of ~2.4. Al-Yaarubi et al. (2005)[12] also reported the LCL model's estimation was about 1.2–1.4 times the hydraulic tests. They used 2 cm × 2 cm transparent replicas of the natural fractures in sandstone, and aperture distribution was estimated by measuring fracture wall geometries at both side of the fracture wall.

In addition, several numerical examinations have been reported based on the fluid-dynamics Navier-Stokes equation. These studies applied a virtual fracture pattern of the sine curve constant wave length. Results showed that compared to these simulations, the LCL model approximation overestimated the flow through the fracture [13,14], increasing the ratio maximum value to minimum one of aperture. Mourzenko et al. (1995)[15] also examined the numerically generated fractures using the Stokes equation and showed that the flow rate through the fractures calculated by LCL was twice that calculated by the Stokes equation. Brush and Thomson (2003)[14] also applied the Navier-Stokes equation to the numerical fracture model to compare with simulations using the LCL model. It was reported that the LCL model was appropriate if the criteria, which is the ratio of the standard deviation to the mean aperture, was even smaller than 1.0. Al-Yaarubi et al. (2005)[12] used a 2 cm sandstone replica sample for the hydraulic test and

measured topographical fracture wall data employing the LCL model simulations. A numerical simulation employing the Navier-Stokes equation was also conducted to compare with the LCL model results and was found to be identical to the hydraulic test of the replica sample; however, the flow rate estimated from the LCL model was larger than both of them. They also compared both simulations by changing the mean aperture of the fracture model and reported that the differences between the Navier-Stokes and the LCL simulations were correlated to the ratio of mean and standard deviation of aperture and the differences ranged from 10% to 100%.

Summarizing, the LCL numerical simulations tend to overestimate the average permeability of fractures correlated to the relative variability of fracture aperture. The variety of fracture aperture definitions, with their different spatial resolutions for measuring aperture, causes the difference between hydraulic tests and the LCL model numerical simulations: vertical aperture, which is a vertical width between upper fracture wall and lower fracture wall; perpendicular aperture, which is perpendicular to fracture wall [16]; ball aperture, which is defined by minimum distance between fracture walls [15]; and segment aperture, which is the average value within a constant range defined by the correlation length of aperture distribution [17]. The tortuosity caused by the undulation of rough fracture walls might be one of the potential reasons of inconsistency between the LCL model and hydraulic test results. Additional work to obtain more quantitative geometrical properties of fracture void space relevant to hydraulic and transport properties is needed. It is worth emphasizing that the limited available data show a lack of correlation between effective apertures based on hydraulic flow and transport measurements.

This study focuses on measuring quantitatively fracture aperture distribution in spatially high resolution under the same hydraulic test and tracer test conditions through the fracture. Various methods for measuring aperture have been reported, including estimating profilometer measurements of both upper and lower fracture walls, the direct measurement of aperture at each sliced or ground cross-sectional surface perpendicular to the fracture, the non-distractive methods of x-ray computed tomography (x-ray CT) or magnetic resonance imaging (MRI). The profilometer method can measure the geometry of fracture walls with both high spatial resolution and high accuracy, but the accuracy of aperture distribution fully depends on one of the reproducibility of superposing upper and lower fracture walls. The cross-sectional surface method also can measure aperture with high spatial resolution and high accuracy for each surface, but the spatial resolution depends on slicing or grinding resolution. The x-ray CT and MRI is useful for investigating microscale aperture without destroying the fracture and can be applicable for the same conditions as

hydraulic tests and tracer tests. However, they need advanced technologies to measure the apertures at scales from several centimeters to several tens of centimeters fractures. Although the optical measurement method has the disadvantage that it requires a transparent replicas of the fractures, it can measure aperture distribution at high spatial resolution and high accuracy under the same conditions as hydraulic tests and tracer tests. In addition, during the tracer tests, the tracer concentration distribution and time-dependent concentration change can investigate quantitatively. The optical measurement method was proposed and applied to fracture aperture measurement by Glass and Tidwell (1991)[18], and it was then used to examine the accuracy of quantitative aperture measurement by applying it to test fractures constructed by textured glass plates [19]. The optical method has the advantage of being able to measure quantitatively both fracture aperture distribution and groundwater flow behavior within the in-plane heterogeneity of a fracture, under the same conditions.

In this study, we applied the optical measurement method to measure both aperture distribution and tracer migration behavior in a transparent replica fractures, duplicating artificially generated tensile fractures in 10 cm of rock block, to obtain data for studying the correlation between effective apertures based on hydraulic flow and transport measurements. The confidence of obtained data in this study was checked by comparing the representative aperture values evaluated from the multiple different measurements, such as aperture distribution measurement and tracer concentration distribution measurement. The aperture data obtained from optical measurement and hydraulic test data was also used for verifying the applicability the LCL model simulations as discussed above.

2. OPTICAL MEASUREMENT SYSTEM

2.1 Basic Theory

The theory of light absorption is used to measure both aperture and dye concentration [9,19]. Light intensity, I , is attenuated depending on the light absorbance of dye, dye concentration, and thickness filled with absorbing dye tracer as the light passes through it, which is the so-called Lambert-Beer law, as formulated below:

$$I = I_0 e^{-\varepsilon_d c_d b} \quad (1)$$

where I_0 is the incident light intensity, ε_d is absorption coefficient of solute (which is dye tracer in this study), c_d is dye concentration, and b is the thickness of dye tracer, which is the fracture aperture in this study. The ratio of light intensity attenuation between the case of filled with dye fluid and filled with water can be written as

$$\ln\left(\frac{I_{\text{dye fluid}}}{I_{\text{fluid}}}\right) = -\varepsilon_d \cdot c_d \cdot b \quad (2)$$

where $I_{\text{dye fluid}}$ is light intensity filling a fracture with fluid that is dyed, I_{fluid} is light intensity filled with non-dyed fluid, such as water, and $\ln(I_{\text{dye fluid}}/I_{\text{fluid}})$ is so-called absorbance. When the correlation between the absorbance and aperture is measured by using a known aperture field, the parameter of $\varepsilon_d c_d$ can be determined. The quantitative fracture aperture field can be calculated by measuring the light absorbance after filling the transparent fracture specimen with both non-dyed fluid and constant concentration dyed fluid. After getting the aperture distribution, the fracture can be replaced with water, and the dyed water is allowed to flow in from one side. Then, it is possible to use an optical measurement system for visualizing dye tracer migration and for measuring dye concentration distribution and time-dependent concentration change at every point, quantitatively. The normalized dye tracer concentration at arbitrary time, at each point in the fracture plane, can be written as:

$$\frac{c_t}{c_0} = \frac{\ln\left(\frac{I_{\text{dye-c}_t}}{I_{\text{water}}}\right)}{\ln\left(\frac{I_{\text{dye-c}_0}}{I_{\text{water}}}\right)} \quad (3)$$

where c_t is dye tracer concentration at time t , c_0 is a constant concentration of dye tracer, I_{water} is transmitted light intensity filling a void space with water, $I_{\text{dye-c}_t}$ is transmitted light intensity filling a void space at time t with migrated dye tracer, $I_{\text{dye-c}_0}$ is transmitted light intensity filling a void space at a constant concentration c_0 of dye tracer.

2.2 Measurement System

The system consists of a transparent replica of a single fracture and a transmitted-light optical measurement system. The fracture replica is made by duplicating a tensile fracture that has been artificially generated in 10 cm of rock block with transparent resin. The optical measurement system consists of a light source of constant intensity (LED Flat light) and a high resolution and sensitive CCD (Charge Coupled Device) sensor to measure the transmitted light intensity through the transparent replica perpendicular to its plane, as shown in Figure 1. The accuracy of optical measurement is strongly dependent on the CCD sensor capability, such as the pixel numbers affecting on the spatial resolution, and the gradation of measuring light intensity. In this study, the DVC-1412AM CCD sensor is used, which is capable of measuring light intensity in 1,392 pixels \times 1,040 pixels and to record in 12 bit (4096 gradation). A band path filter (central wavelength of 510 nm, half bandwidth of 10 nm) is also used to measure monochromatic light intensity for applying Lambert-Beer's law.

2.3 Transparent Replica Specimen of a Single Fracture

In this study, transparent replica specimens of a single fracture are made by duplicating a tensile fracture that has been artificially generated in granite block at 100 mm with transparent resin. The tensile fracture was generated in ~10 cm × 10 cm × 10 cm cubic granite block. The rock is composed of mainly quartz, feldspar, K-feldspar, and biotite, and grain size varies from about 2 to 4 mm [20]. Both sides of the fracture walls are molded in silicone resin, and a replica of each fracture wall is copied by transparent epoxy resin (Nissin Resin Co Ltd, Crystalresin II). The injection and withdrawal ports are attached at both ends of the transparent fracture specimen, and the other sides are fixed as no-flow boundaries, as shown Figure 2.

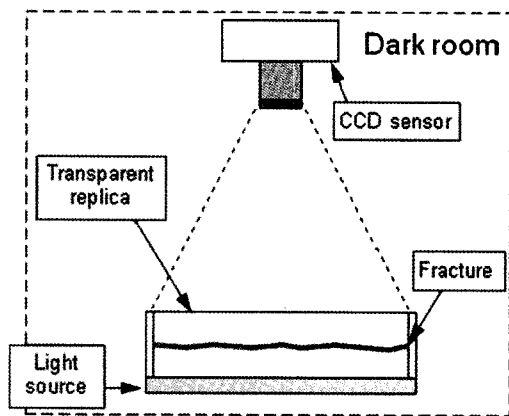


Fig. 1. Concept of an Optical Measurement System in a fracture. Transmitted Light Intensity Passing through the Fracture is Measured by CCD Sensor

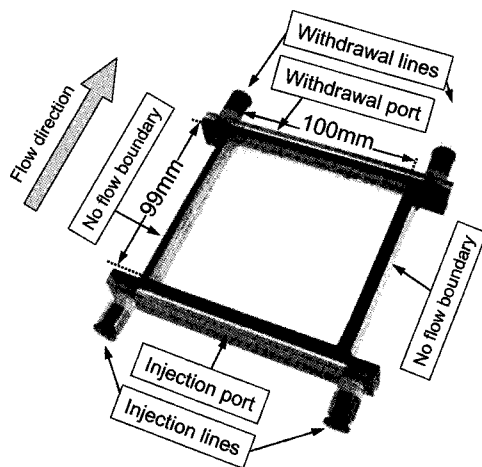


Fig. 2. An Example of a Transparent Replica Specimen of a Single Fracture. The Injection and Withdrawal Ports are Attached at both Ends, and the Other Sides are Fixed as No-flow Boundaries

3. EXPERIMENTAL RESULTS

3.1 Aperture Measurement

The aperture distribution can be measured by using the correlation between absorbance and fracture width, as described in Equation (2). The parameter, $\epsilon_d C_d$, was calibrated by using a transparent fracture specimen that has known aperture field. The known aperture transparent specimen for the calibration had a wedge structure, made by two flat glass plates (100 mm × 100 mm) with contact on one side and holding a certain aperture by a fixed spacer on the other side, as shown in Figure 3. The wedge shape void space was filled by constant concentration of dyed fluid. The surface accuracy of the flat glass plate was 0.00063 mm in 100 mm × 100 mm square. Figure 4 is an example of the calibration result showing the correlation between the light intensity ratio and aperture. With the measured data at 0.0026 mm increments of aperture in the range of 0.1 mm to 2.20 mm, about 770 data points are plotted in Figure 4, which follows the linearity of Equation (2), and from the regression line, $\epsilon_d C_d$ of Equation (2) can be calibrated as 0.733 in the case of Figure 4.

We observed the light intensity through the transparent replica in both the case of the filling non-dyed fluid and the case of the dyed fluid with constant concentration dye. Then, the fracture aperture distribution was calculated by using the correlation between the light intensity ratio and aperture, as shown in Figure 4. In this study, for aperture measurement, a fluid with similar refraction coefficient to the transparent resin was used for both the wedge shape fracture sample and a transparent replica fracture specimen in order to avoid the refraction effect from transmitting light through the boundary between transparent resin and water. Figure 5 shows the calculated aperture distribution, with high spatial resolution in 958 pixels by 958 pixels of

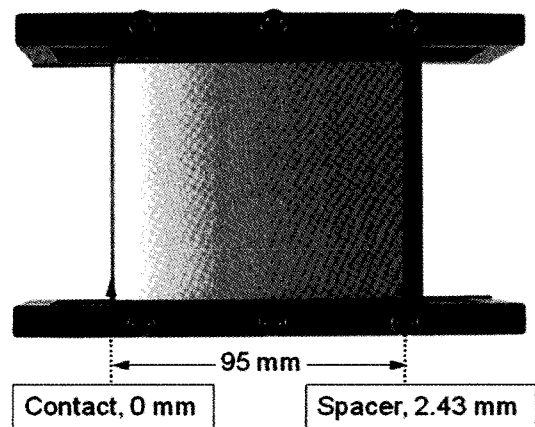


Fig. 3. An Example of Wedge Shape Fracture, Top View. The Specimen was Made by Two Glass Plates with Contacting Left Sides and Holding a 2.43 mm by a Spacer at the Right Side. The Wedge Shape Space was Filled by Constant Concentration of Dyed Fluid

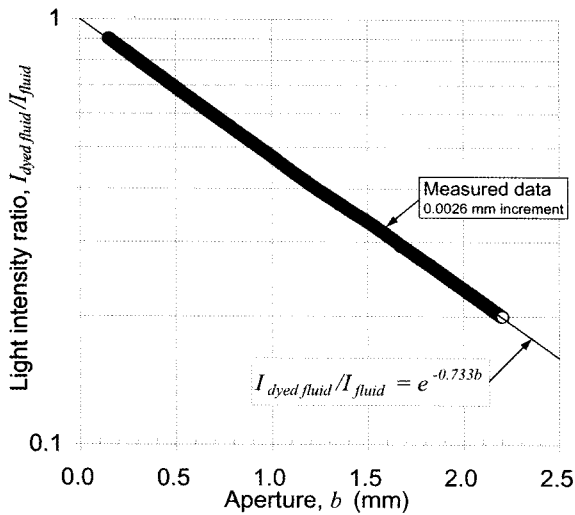


Fig. 4. An Example of Correlation between Light Intensity Ratio and Aperture. Open Circles are the Measured Data in 0.0026 mm Increments of Aperture in the Range of 0.10 mm to 2.20 mm; the Line Shows Regression Line to the Data

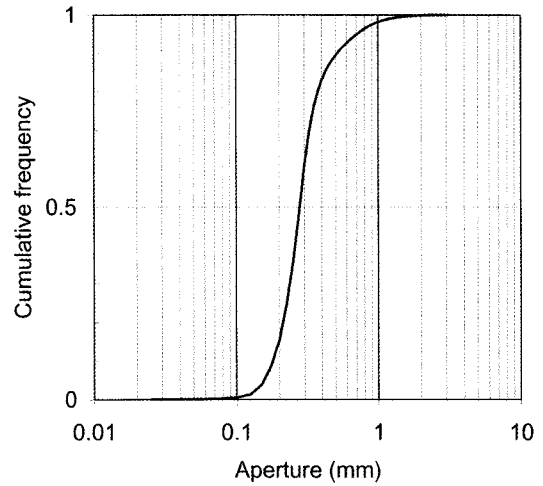


Fig. 6. Cumulative Frequency of Aperture Distribution as Shown in Figure 5

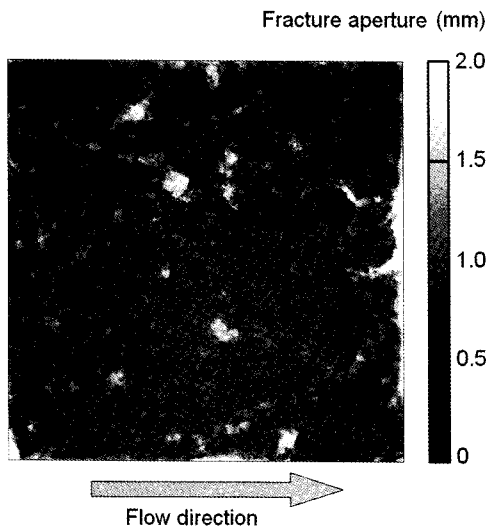


Fig. 5. An Example of Fracture Aperture Distribution by the Transmitted Light Optical Method of the Transparent Fracture Replica

100 mm × 99 mm size of the transparent replica. Spatial resolution for the measurement is about 0.10 mm in this study. Figure 6 shows the cumulative frequency of measured aperture distribution. Because the fracture was artificially generated in tensile condition, there might not be anisotropic distribution of aperture, such as striation caused by shear displacement of the fractures. From Figure 5, the fracture aperture seems to be randomly distributed in space. An arithmetic average and the standard deviation of aperture are 0.33 mm and 0.20 mm, respectively. Total void volume

of the fracture was also measured by comparing the weight of the transparent replica specimen with and without water under constant temperature. The measured fracture void volume was 3,460 mm³. The average aperture estimated from the total void volume is 0.35 mm, which is close to the arithmetic mean of the aperture distribution measured by the transmitted light optical method.

3.2 Hydraulic Test

The hydraulic characterization, transmissivity, of the transparent fracture was measured by the hydraulic test using a one-way flow direction, as shown in Figures 2 and 5. The water employed in this study was prepared by degassing distilled water and equilibrating it in room temperature, at about 20 degree centigrade. A nonpulsation double plunger pump was used to maintain constant flow injection into the fracture. The head difference between injection and withdrawal port was directly compared by the piezometers connecting each port. Figure 7 shows the result of the hydraulic test, the relationship between hydraulic gradient and flow rate through the fracture, and Reynolds number, Re . With the Reynolds number ranging from 0.3 to 1.5, the hydraulic tests were conducted at conditions of around $Re = 1$, which is slightly larger than the Reynolds lubrication criterion, $Re < 1$ [21]. The hydraulic aperture calculated from Figure 7 and the cubic law was about 0.24 mm (standard deviation: 0.0018 mm).

3.4 Tracer Test

The tracer test was conducted by using a constant concentration dye tracer under the constant flow rate, 3.3 mm³/s, with the same flow direction as the hydraulic tests. The Reynolds number at this flow rate is 0.03. The water at the injection port (Figure 2) was replaced with the dye tracer before starting the tracer inlet. Every 30

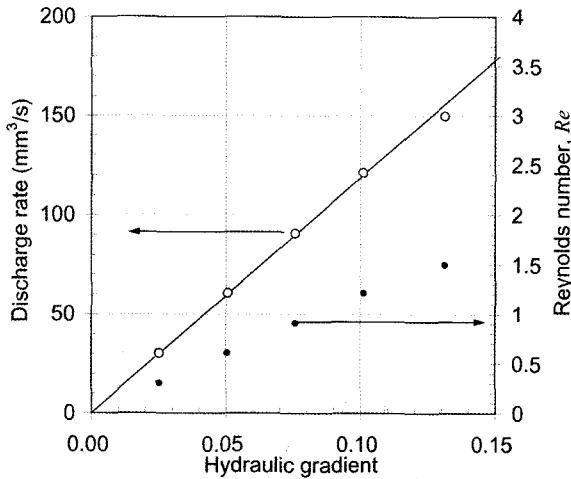


Fig. 7. Hydraulic Tests Results for the Transparent Fracture Replica Specimen. Open Circles Show the Measured Flow Rate, a Solid line Shows the Regression of Open Circles, and Solid Circle Shows Reynolds Number

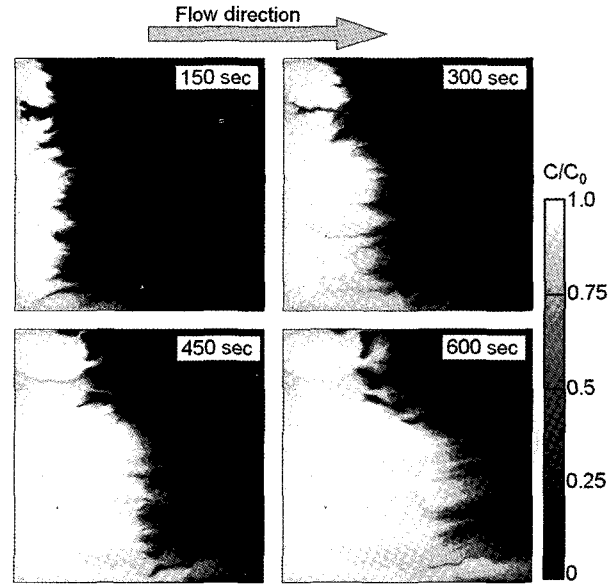


Fig. 8. An Example of Tracer Concentration Measured by Transmitted Light Optical Method during the Tracer Migration Test of Dye Tracer. Heterogeneous Distribution of Flow Paths and Tracer Migration could be Visualized, and Quantitative Concentration of Tracer Distribution could be Obtained

seconds the light attenuation by the dye tracer migration was measured by CCD sensor. Figure 7 shows an example of the distribution of dye tracer, represented by concentration ratio normalized by inlet dye tracer concentration, evaluated by Equation (3). The spatial resolution is the same as aperture distribution measurement. This data set, quantitative aperture distribution, and tracer concentration are valuable not only for visualizing advection dispersion phenomena in a variable aperture fracture, but also for validating any numerical codes for advection dispersion transport in heterogeneous flow fields. From the quantitative concentration distribution at each 30 seconds, the tracer breakthrough curve in the fracture in the vicinity of the withdrawal port could be evaluated. This breakthrough curve does not include any dispersion effects by the dead volume in the withdrawal port, tubing, and sensor ports for measuring tracer concentration. Figure 9 shows cumulative breakthrough curves for tracer mass normalized by the amount of injected tracer concentration in the case of pulse injection. The mean residence time, t_m [22] of the tracer breakthrough is calculated by

$$t_m = \int_b^{\infty} \frac{C(\infty) - C(t)}{C(\infty)} dt \quad (4)$$

where $C(t)$ is breakthrough tracer concentration at time t . The mean residence time calculated from the tracer breakthrough curve as shown in Figure 9 is 1033 seconds. The mass-balance aperture, b_m , which is the representative aperture contributing to mass transport, is also calculated by

$$b_m = \frac{Q \cdot t_m}{L \cdot W} \quad (5)$$

where Q is water flow rate through the fracture, L is fracture length (99 mm in this study) and W is fracture width (100 mm in this study). The mass-balance aperture is evaluated from the flow rate, 3.3 mm³/s, and the mean residence time, 1033 seconds. The evaluated aperture value is 0.35 mm, which is equal to the average aperture estimated from fracture void volume measurement, and is close to the arithmetic mean of aperture measured by the transmitted light optical method, as described in Section 3.1. The mass-balance transport aperture evaluated from this tracer test is the total void volume for contributing to the tracer transport. As shown in Figure 8, most of the area of the fracture might contribute to tracer transport during the tracer test. There might not be significant dead volume for the tracer migration. This is one of the reasons for the convergence between two aperture values – a good agreement between two different measuring values, which indicates the accuracy of this study for both aperture measurement and tracer breakthrough concentration.

4. DISCUSSION

The aperture distribution measured by the optical measurement was compared with the hydraulic test results. In general, the spatially random distributed flow field, the representative hydraulic conductivity, can be estimated from the geometrical mean of hydraulic conductivity [7,8]. As shown in Figure 5, in this study, fracture aperture

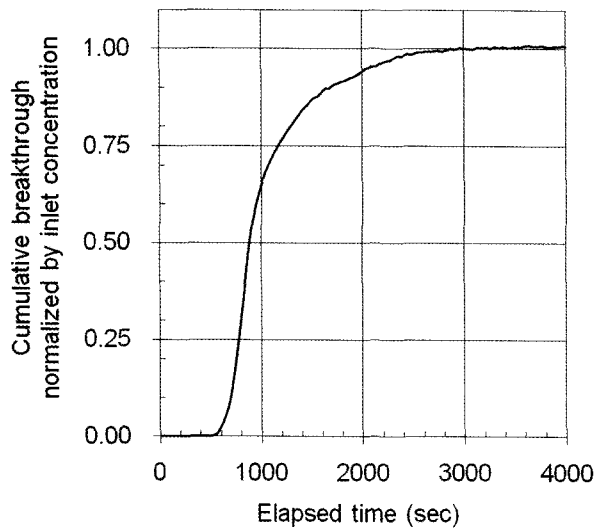


Fig. 9. Tracer Breakthrough Curve Evaluated in the Fracture in the Vicinity of Outlet port. The Breakthrough Curve was Normalized by Inlet Concentration

tends to be randomly distributed. The geometrical mean of the aperture, 0.29 mm, might be one of the indicators for estimating representative hydraulic property, transmissivity. Table 1 summarizes each representative value of fracture aperture estimate from the different measures. The geometrical mean aperture is relatively larger than the hydraulic aperture estimated from the hydraulic test and cubic law. However, the aperture values evaluated from the multiple different measurement methods, arithmetic mean of aperture distribution measured by the optical method, transport aperture evaluated from the tracer test, and average aperture evaluated from fracture void volume measurement, converged to a unique value, which indicates the accuracy of this experimental study.

The aperture data was also employed for the numerical simulation. The aperture value at each measured point was translated to transmissivity based on the cubic law, under the assumption of LCL. The translated transmissivity field, the LCL model, was used in the finite element code of two-dimensional Darcy flow simulation code, MAFIC [23], under a steady state and saturated conditions. The flow rate calculated by the LCL model is compared with the hydraulic tests, as shown in Figure 10. In this figure, the flow rate estimated from geometric mean aperture with cubic law is also plotted to compare with the LCL model simulation. From this figure, the LCL model simulation tends to overestimate flow rate through the fracture. This is consistent with results from previous studies as summarized in above.

5. SUMMARY

Experimental examinations for evaluating fracture

Table 1. The Representative Fracture Aperture Estimated from the Different Measures

Estimation method	Aperture (mm)
Hydraulic aperture estimated from hydraulic test and cubic law	0.24
Arithmetic mean of aperture distribution measured by the optical method	0.33
Geometrical mean of aperture distribution measured by the optical method	0.29
Transport aperture evaluated from the tracer test	0.35
Average aperture evaluated from fracture void volume measurement	0.35

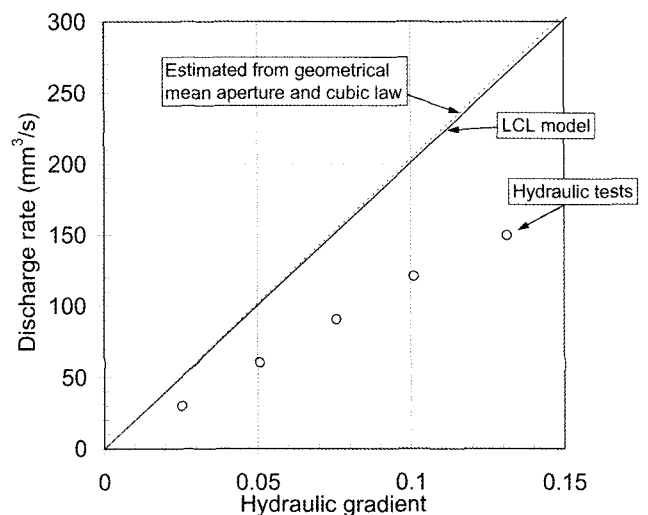


Fig. 10. Comparison Numerical Simulations with LCL with Hydraulic Test Results. Open Circles Show the Hydraulic Results, Which are Same as Figure 7. The Solid Line is the Numerical Simulation Results of the LCL Model. The Broken Line is the Discharge Rate Estimated from the Cubic Law of Geometric Mean Aperture

characteristics were conducted by using a transparent replica of a single fracture. Quantitative aperture distribution with high spatial resolution was obtained by measuring the attenuation of transmitted light through the fracture. A hydraulic test was also conducted for the fracture replica specimen in a single direction of flow. Applying transmitted light optical measurement, the tracer concentration in the fracture could be quantitatively measured. From the quantitative tracer concentration data at each point in time, a breakthrough curve for the fracture in the vicinity of the withdraw port was also obtained, which was undisturbed by the dispersion effect of relatively larger volume for the port and/or any kind of sensors for measuring tracer

concentration. The transport aperture was evaluated from mean residence time calculated from the breakthrough curve. Results from the various representative aperture values – (1) arithmetic mean aperture; (2) geometric mean aperture; (3) hydraulic aperture calculated from the hydraulic tests and cubic law; and (4) transport aperture evaluated from the tracer test – were all evaluated. The numerical analysis for simulating flow through the fracture was also conducted after translating aperture data to transmissivity field data by cubic law under the assumption of LCL. The evaluated flow rate was larger than the hydraulic tests. This result is consistent with previous studies showing that the LCL model might calculate a 10% – 100% larger discharge rate than hydraulic tests. This disjunction between hydraulic test data and the LCL model results from spatially high-resolution aperture measurement data might result from the spatial frequency of aperture variations or from local inertial effects, although solutions should await further studies – not only any experimental examinations for accumulating data, but also any numerical simulations for fluid dynamics in fractures with a fully heterogeneous aperture field. This experimental study might contribute to the data set of quantitative aperture measurement data with flow and transport tests data used for further numerical examinations. In addition, more advanced numerical simulations of water fluid dynamics in fully heterogeneous aperture fields in fractures should be compared with the experimental data obtained in this study.

REFERENCES

- [1] JNC, H12: Project to Establish the Scientific and Technical Basis for HLW Disposal in Japan, Project Overview Report, Second Progress Report on Research and Development for the Geological Disposal of HLW in Japan, JNC TN1410 2000-001, 2000.
- [2] Silliman, S. E., An Interpretation of the Difference Between Aperture Estimates Derived From Hydraulic and Tracer Tests in a Single Fracture, *Water Resour. Res.*, Vol.25, No.10, pp.2275-2283, 1989.
- [3] Tsang, Y. W., Usage of “Equivalent Aperture” for Rock Fracture as Derived From Hydraulic and Tracer Tests, *Water Resour. Res.*, Vol.28, No.5, pp.2033-2048, 1992.
- [4] Tsang, Y. W., and C. F. Tsang, Hydrological characterization of variable-aperture fractures, in *International Symposium on Rock Joints*, pp. 423-430, A. A. Balkema, Brookfield, Vt., 1990.
- [5] Unger, A. J. A., and C. W. Mase, Numerical study of the hydromechanical behavior of two rough fracture surfaces in contact, *Water Resour. Res.*, Vol.29, No.7, pp.2101-22114, 1993.
- [6] Louis, C., A Study of groundwater flow in jointed rock and its influence on the stability of rock masses, *Rock Mech, Res Rep.* No.10, 1969.
- [7] Smith, L., and R. A. Freeze, Stochastic Analysis of Steady State Groundwater Flow in a Bounded Domain, 2. Two-Dimensional Simulations, *Water Resour. Res.*, 15(6), 1543-1559, 1979.
- [8] Dagan, G., Models of groundwater flow in statistically homogeneous porous formations, *Water Resour. Res.*, 15(1), 47-63, 1979.
- [9] Nicholl, M. J., H. Rajaram, R. J. Glass, and R. Detwiler, Saturated flow in a single fracture: Evaluation of the Reynolds equation in measured aperture fields, *Water Resour. Res.*, Vol.35, No.11, pp.3361-3373, 1999.
- [10] Konzuk, J. S., and B. H. Kueper, Evaluation of cubic law based models describing single-phase flow through a rough-walled fracture, *Water Resour. Res.*, Vol.40, W02402, 2004.
- [11] Hakami, E., and E. Larsson, Aperture measurements and flow experiments on a single natural fracture, *Int. J. Rock Mech. Miner. Sci. Geomech. Abstr.*, 33(4), 395-404, 1996.
- [12] Al-Yaarubi, A. H., C. C. Pain, C. A. Grattoni, and R. W. Zimmerman, Navier-Stokes Simulations of Fluid Flow Through a Rock Fracture, *Dynamics of Fluids and Transport in Fractured Rock*, Faybishenko et al, ed., AGU, pp.55-64, 2005.
- [13] Brown, S. R., H. W. Stockman, and S. J. Reeves, Applicability of the Reynolds Equation for Modeling Fluid Flow between Rough Surfaces, *Geophys. Res. Lett.*, 22(18), 2537-2540, 1995.
- [14] Brush, D. J., and N. R. Thomson, Fluid flow in synthetic roughwalled fractures: Navier-Stokes, Stokes, and local cubic law simulations, *Water Resour. Res.*, 39(4), 1085, doi:10.1029/2002WR001346, 2003.
- [15] Mourzenko, V. V., J. F. Thovert, and P. M. Adler, Permeability of a Single Fracture; Validity of the Reynolds Equation, *J. Phys. II France* 5, 465-482, 1995.
- [16] Ge, S., A governing equation for fluid flow in rough fractures, *Water Resour. Res.*, Vol. 33, No.1, 53-61, 1997.
- [17] Oron, A. P., and B. Berkowitz, Flow in Rock Fractures, The Local Cubic Law Assumption Reexamined, *Water Resour. Res.*, Vol.34(11), 2811-2825, 1998.
- [18] Glass, R. J., and V. C. Tidwell, Research program to develop and validate conceptual model for flow and transport through unsaturated, fractured rock, paper presented at 2nd International Conference of High Level Radioactive Waste Management, Am. Nucl. Soc., Las Vegas, Nev., April 28 to May 3, 1991.
- [19] Detwiler, R. L., S. E. Pringle and R. J. Glass, Measurement of fracture aperture fields using transmitted light: An evaluation of measurement errors and their influence on simulations of flow and transport through a single fracture, *Water Resour. Res.*, Vol.35, No.9, pp.2605-2617, 1999.
- [20] Lin, W., Ohta, Y., Takahashi, M., Sugita, N, Effect on Strain Rate on Compressive Strength and Deformability of Granite, *Shigen to Sozai*, Vol. 118, No. 5,6 pp.377-384, 2002
- [21] Zimmerman, R. W., and G. S. Bodvarsson, Hydraulic Conductivity of Rock Fractures, *Transport in Porous Media*, 23:1-30, 1996.
- [22] Moreno, L., Y. W. Tsang, C. F. Tsang, F.V. Hale, and I. Neretnieks, Flow and Tracer Transport in a Single Fracture: A Stochastic Model and Its Relation to Some Field Observations, *Water Resour. Res.*, Vol.24, No.12, pp.2033-2048, D 1988.
- [23] Miller I., G. LEE, and W. Dershowits, MAFIC User documentation, Golder Associates Inc., Redmond, Washington, USA, 2001.